

A Compact Ocean Bottom Electromagnetic Receiver and Seismometer

Kai Chen¹, Ming Deng¹, Zhongliang Wu², Xianhu Luo², Li Zhou¹

¹School of Geophysics and Information Technology, China University of Geosciences (Beijing),
5 Beijing, China

² MLR Key Laboratory of Marine Mineral Resources, Guangzhou Marine Geological Survey, Guangzhou,
China

Correspondence to: Kai Chen (ck@cugb.edu.cn)

Abstract. Joint marine electromagnetic (EM) and seismic interpretation are widely used for offshore
10 gas hydrate and petroleum exploration, produce better estimates of lithology and fluids, and decrease
the risk of low gas saturation. However, joint data acquisition is not commonly employed. Current
marine EM data acquisition depends on an ocean bottom electromagnetic receiver (OBEM) and current
seismic exploration methods use seismometers. Joint simultaneous data acquisition can decrease costs
and improve efficiency; yet conventional independent data receivers have several drawbacks, including
15 large size, high costs, position errors, and low operational efficiency. To address these limitations, we
developed a compact ocean bottom electromagnetic receiver and seismometer (OBEMS). Based on
existing ocean bottom E-field receiver (OBE) specifications, including low noise levels, low power
consumption, and low clock-drift error, we integrated two induction coils for the magnetic sensor and a
three-axis omnidirectional geophone for the seismic sensor and assembled an ultra-short base line
20 (USBL) transponder as the position sensor, which improved position accuracy and operational
efficiency while reducing field data acquisition costs. The resulting OBEMS has a noise level of 0.1
nV/m/rt (Hz) at 1 Hz in E-field and 0.1 pT/rt (Hz) at 1 Hz in B-field and a 30 day battery lifetime. It
also supports a WiFi interface for configuring data acquisition parameters and data download. Offshore
acquisition was performed to evaluate the system's field performance during offshore gas hydrate
25 exploration. The OBEMS functioned effectively throughout operation and field testing. The OBEMS
therefore functions as a low cost, compact, and highly efficient joint data acquisition method.

1 Introduction

Marine electromagnetic (EM) and seismic methods are important geophysical tools used for offshore
petroleum exploration (Barsukov and Fainberg, 2017; Constable and Srnka, 2007; Ellingsrud et al.,
30 2002), gas hydrate mapping (Schwalenberg et al., 2017; Weitemeyer et al., 2006), physical
oceanography (Zhang et al., 2014), crustal studies (Constable and Heinson, 2004; Key and Constable,
2002; Kodaira et al., 2000), mid-ocean ridge studies (Key, 2012), subduction zone studies (Naif et al.,
2015), and underwater target detection (ISL, 2016). To improve interpretation accuracy, and decrease
the risks associated with offshore drilling, increasingly more surveys are conducting multi-physics
35 integrated interpretation and cooperative inversion, such as marine EM and seismic joint interpretation
(Goswami et al., 2015; Goswami et al., 2017; Weitemeyer et al., 2011). In offshore exploration,
seismic and EM data acquisition are typically performed independently. Joint offshore seismic and EM

data acquisition would not only increase efficiency and decrease costs, but also improve interpretation accuracy (Engelmark et al., 2012). Complementary data also enhance our understanding of subsurface characteristics; while seismic methods provide an indication of the subsurface architecture, EM is more sensitive to changes in fluids. Seismic data can be inverted for velocity and acoustic impedance, while inversion of EM data provides resistivity values. Correlating these two methods has the potential to improve hydrocarbon saturation estimates and drilling success rates.

Ocean bottom electromagnetic receivers (OBEM) are used to measure seafloor magnetotelluric (MT) and controlled source electromagnetic (CSEM) field signals. The first seafloor EM measurements made using the MT method occurred in the 1960s by Jean Filloux and colleagues (Filloux, 1967). More recently, Scripps Institution of Oceanography (SIO) collaborated with Quasar to design a small EM receiver (QUASAR, 2016) based on the existing SIO EM receiver (Constable, 2013) for compact, low cost EM data acquisition. The resulting QMax EM3 optimized efficiency and safety, enabling survey contractors to achieve faster deployment and recovery times, utilize more receivers, and perform more surveys in a shorter time period (QUASAR, 2016). Kasaya (2009) also developed a small OBEM and ocean bottom electrometer (OBE) system, which had an arm-folding mechanism to facilitate assembly and recovery operations. For magnetic observations, they used a fluxgate sensor. This OBE mainly focuses on marine MT acquisition, and CSEM is not included. Current trends in instrumentation involve smaller sizes, lower power consumption, lower noise levels, and lower data acquisition costs. Marine EM field data acquisition technology continues to improve, with reduced costs and increased flexibility.

Ocean bottom seismometers (OBS) have been employed to produce offshore seismographs since the 1970s. OBS are usually equipped with three component geophones to record the sound waves generated by either earthquakes at depth or man-made devices near the surface. They record the movement of the seafloor in all directions while a hydrophone records the pressure in the surrounding water. The French Research Institute for Exploitation of the Sea (IFREMER) (Auffret et al., 2004) developed a new generation of ocean bottom seismometers by integrating acquisition and instrument release, adding a rechargeable battery, enabling data downloads by a USB cable, and reducing the unit's size. GeoPro GmbH developed a similar system where the CPU and recorder are housed in a 17-inch glass sphere. Panahi et al. (2008) designed a low power data logger for OBS systems based on a compact flash card. Sercel and Geopro are currently the leading manufacturers in the OBS market; all their instruments are designed for low power consumption, low noise levels, low time drift error, and a compact size.

Marine controlled-source electromagnetic (CSEM) sounding is a new tool available to geophysicists for offshore gas hydrate exploration (Weitemeyer, 2011). And the technique has been developed for the detection of deep hydrocarbon reservoirs (Fanavoll, 2010). The OBEM is the receiver which measure the EM field for the marine CSEM or/and MT method. OBS mainly provides deep geological information, and it also used to shallow gas hydrate mapping (Mienert, 2005). Therefore, these two offshore active/passive geophysical explorations instrument could jointly provide a complementary image to identify natural resources and/or geology structure. Thus, join the OBEM and OBS data

acquisition to investigate gas hydrate or petroleum exploration within a few kilometers below seafloor is available.

80 Current offshore EM and seismic data acquisition usually employ both OBEM and OBS, but the two instruments operate independently. There are two disadvantages to independent data acquisition: 1) the error related to each individual instrument position; and 2) the cost of offshore data acquisition, which includes instrument hardware, research vessels, human resources, etc. Considering the former, the quality of marine CSEM data is dependent on accurate navigational information for both transmitter and receiver positions and orientations. Current OBEMs locate by acoustic release, which has a larger
85 position error, and uses the near field to refine the geometry of the transmitter and receiver locations (Weitemeyer, 2011), which are dependent on data post-processing. Position errors may lead to reduced inversion accuracy.

KMS and GeoSYN developed a GEOSYN/KMS 870-VectorSeisEM Broadband-Ocean bottom station, which is a broadband 4C seismic/6C electromagnetic node for shallow and deep water geophysical
90 applications. Using a single survey vessel, Petroleum Geo-Services Inc. can acquire high-density EM data simultaneously with 2D GeoStreamer® seismic data, or high-density 3D EM data over existing, or planned 3D seismic data. Offshore high-density joint EM and seismic acquisition and integrated data analysis represents a stepwise change in the application of EM technology. Both technologies seek to mitigate risk when searching for and extracting oil and gas. During 2010, we acquired coincident
95 marine CSEM and OBS data when PGS conducted one of the first field trials of their towed streamer EM system at the Troll field in the Norwegian North Sea (Zhdanov et al. 2012). The towed-streamer EM system allows CSEM data to be acquired simultaneously with seismic data over very large areas, resulting in higher production rates and lower costs than for conventional CSEM acquisition.

China University of Geosciences (Beijing) (CUGB) developed an OBEM in 1998 (Deng et al., 2003).
100 During the past 20 years, CUGB has successfully used its OBEM equipment in deep EM surveys for gas hydrate mapping and hydrocarbon exploration (Wei et al., 2009; Jing et al., 2016). The OBEM has also been widely used for marine magnetotelluric and CSEM measurements. The current OBEM system has an acoustic telemetry modem and folding-arm mechanism (Chen et al., 2015), with low noise levels and low time drift errors. In 2014, CUGB developed a micro OBE for low cost and highly
105 efficient data acquisition (Chen et al., 2017). To achieve joint EM and seismic data acquisition, the instrument was upgraded from an existing micro OBE by: 1) integrating a three-axis omni-directional geophone for seismic parameter measurements; 2) installing two induction coils for horizontal magnetic field component measurements; and 3) installing an ultra-short baseline (USBL) transponder for tracking seafloor position as the system ascends after release.

110 The OBEMS has been mechanically optimized to satisfy all technical requirements for simultaneous joint seismic and electromagnetic data acquisition. This technical advancement permits enhanced modeling and simultaneous interpretation of both datasets, which minimizes acquisition costs. The advantages of this OBEMS include 1) lower cost and higher efficiency of both the instrument and offshore data acquisition, as the same cost includes more nodes needed to improve horizontal
115 resolution and 2) a smaller seafloor instrument position error, which decreases the inversion error. The OBEMS system can also replace an OBEM as the receiver in marine CSEM surveys. In addition, the

OBEMS can be used for OBS observations. In the future, a hydrophone will be added to the OBEMS system to allow measurement of the acoustic pressure field.

2 Instrument specifications

120 To achieve joint EM and seismic data acquisition with the goals of reducing the data acquisition cost and improving operational efficiency, we developed a new OBEMS. The OBEMS was then used to record seafloor EM field and motion signals. Figure 1 shows a schematic of the system. The OBEMS consists of a nylon frame, two glass spheres, a red flag, a transducer, a USBL transponder, a data logger, a battery, three geophones, four electrodes, two induction coils and an anchor. The equipment is
125 fixed on a nylon frame measuring $105\text{cm} \times 55\text{cm} \times 65\text{cm}$. All electronics are installed inside a 17-inch glass sphere except the transducer and USBL, while the other glass sphere provides buoyancy. Figure 2 show the photo of the OBEMS while floating up on sea level. We used Ag/AgCl electrodes to measure the electric voltage in the Ex dipole and Ey dipole. The E-field noise level was 0.1 nV/m/rt (Hz) at 1 Hz (at a working water depth of 1000m) with a 12m dipole. Three 8 Hz omni-directional geophones
130 were used as seismometer to record artificial earthquakes signal. The moving coil geophone may generate EM noise for magnetic sensors, but the electronics (data acquisition circuit board, battery and geophone) are all shield by ferrite film, and the distance between induction coil and geophone is too large to measure the EM noise. We confirm the EM noise of geophone test in magnetic shield room. The geophone sensitivity is 78.5 V/m/s at a 15 Hz natural frequency, and the internal
135 resistance is 3100Ω . Four sets of six 18650 Li-ion batteries for 25.2 V batteries supply power to the data logger circuit. One independent 16.8 V battery supplies the acoustic telemetry modem (ATM) module. The power consumption is approximately 1W. The power supply module supports data acquisition for ~30 days at a maximum sampling rate of 2400 Hz.

The OBEMS data logger has a 24 bit analog-to-digital converter for each of the two electrical field
140 components and the three-axis geophone components. The attitude and heading reference system (AHRS) module records the pitch, roll, and heading while the instrument is on the seafloor. The OBEMS has two parallel release mechanisms. The transducer connects with the ATM for acoustic telemetry. When the ATM receives the release command, the burn-wire mechanism release is driven, and the anchor releases after 10 minutes. Additionally, a USBL transponder responder and motor-
145 driven release were also installed on the OBEMS. The transponder is designed for positioning remotely operated vehicles (ROVs), towed fish, and other mobile targets in water depths up to 4000 m and is equipped with an omni-directional transducer for a wide range of general USBL tracking applications. The transponder is available with acoustically controlled output lines suitable for an external motor drive. This transponder integrated the USBL transponder, release, and the internal depth sensor to
150 improve USBL position performance.

The resulting reduction in positioning uncertainty leads to significant improvements in target sensitivity. Acoustic ultra-short baseline communication (USBL) is used to establish the exact receiver positions. The OBEMS integrated USBL transponder which is from Sonardyne GyroUSBL underwater acoustic positioning solution, and the accuracy is approximately 1.5 % of

155 the slant distance. While the slant distance is 2000m, we estimate that receiver positions obtained
this way are accurate to about 3 m. The OBEM which is from EMGS position is monitored by
acoustic USBL transponders. The OBEM which are from SIO accurate navigational data were
meant to be collected using a short baseline (SBL) acoustic navigation system. They estimate that
receiver positions obtained this way are accurate to about 3-5 m. The USBL is more convenient to
160 install and use than SBL, and the accuracy is enough.

To keep the design of the OBEMS simple and compact, the seismometers were indirectly coupled to
the seafloor via the sphere, release hardware, anchor, and the spring used to connect the OBS to the
anchor. While seismometers work best when they are in direct contact with the Earth (Manuel et al.,
2012), this design has been proven effective in collecting data at long shot-receiver offsets. Coupling
165 the instrument to the seafloor is extremely important, as the geophone, which measures movement of
the seafloor, is located inside the sphere rather than deployed on the seafloor. To further optimize
coupling, a weight in the form of a cross with a U-profile was used to ensure good penetration of the
anchor weight into the seafloor.

To provide the highest possible accuracy, time was recorded to the nearest millisecond. Each OBEMS
170 uses a microprocessor-compensated oscillator (MCXO) as a stable clock reference, for which the drift
can be as little as 2 ms/day. Following each deployment, the offset is measured to compensate for the
total time drift.

The size of the anchor is 110cm x 60cm x 6cm and it weighs 136kg in air and 78kg in water. During
deployment, the weight of the OBEMS in water is 42 kg, and -36 kg when it ascends. The descent and
175 ascent velocities of the OBEMS are approximately 1 m/s and 0.8 m/s, respectively. Table 1 shows the
specifications of the OBEMS system.

3 Electronics

Figure 3 shows a schematic of the OBEMS data logger. The data logger is based on a 24-bit analog-to-
digital converter (ADC) for each channel. Different analog pre-amplifiers were used for electric field,
180 magnetic field, and geophone measurements. The data logger contains eight channels. Each channel
integrates a pre-amplifier and 24-bit ADC. The pre-amplifier for the E-field channel is an ultra-low
noise chopper amplifier; the self-noise level is approximately 0.6 nV/rt(Hz) at 1 Hz, the gain is 1200,
and the -3 dB bandwidth is 100 s to 100 Hz. The pre-amplifier for the geophone is a different amplifier
with a gain of 20 dB. The gain of induction coil is 300mV/nT, and the output range is $\pm 5V$. The input
185 range of the ADC is $\pm 5 V_{pp}$ to match the pre-amplifier and induction coil output range. The ADC
module is based on an eight-channel, 24-bit ADC: the ADS1282. The ADS1282 is a one-channel, high
dynamic range, fourth order Δ - Σ modulator, with a digital filter for data decimation and interfacing
with the microcontroller module which provides a dynamic range of 130 dB at a 250 Hz sample rate,
and a total harmonic distortion (THD) of -122 dB. The full scale of ADC is $\pm 2V$ and the attenuation
190 coefficient is set 0.4.

Micro-control unit (MCU) A is the master MCU, which is used to set sample rate, configure the ADC
register, write data to the SD card, communicate with a computer via a WiFi module, and to

communicate with the slave MCU B, the AHRS module, and the GPS module via a serial port. The complex programmable logic device (CPLD) parallel reads converted data from eight ADCs and series
195 data awaiting MCU A data transfer. The MCU A employs an internal direct memory access (DMA) controller and writes data to the SD card. The MCXO is from Vectron, with a low power consumption of 3.3 V & 12 mA and high frequency stability of approximately ± 20 ppb from 0 °C to 50 °C. The CPLD generates a 2.4576 MHz clock as the ADC master clock. The sampling rate can be set to 2400 Hz, 600 Hz, or 150 Hz.

200 MCU B is used as the slave MCU for communication with ATM, driving the burn wire current source, measuring battery capacity, and as a pressure sensor inside the glass sphere. When the ATM receives the release command, MCU B drives the current source and provides 500 mA to the burn-wire release. A charger module converts the external DC 28V to charge each Li-ion battery set independently. The collected data are stored on an SD card. To download the data there is no need to open the glass
205 sphere or use an Ethernet wire. A computer can connect to the data logger to download data and configure acquisition parameters using the onboard WiFi module. The capacity of the SD card is 32 GB, and can be expanded to 128 GB. The sampling rate was set to 150 Hz, generating 400 MB of data per day. An effective download speed of 3 MB/s was achieved, which allows 30 days of data (approximately 12 GB) to be downloaded in less than 67 min. After the OBEMS has been released
210 from its anchor and is floating at the surface, it can be recovered using radio signals that can be detected by a 165 MHz Very High Frequency (VHF) direction finder at distances of up to 5 km, even in poor visibility. The flashing light inside the sphere is especially useful for recovery at night. Figure 4 shows the Photo of the data logger installed in the glass sphere.

4 Offshore experiments

215 In August 2018, we conducted offshore experiments to map gas hydrates in the Qiongdongnan region of the South China Sea. The support vessel used was the *Hai Yang Si Hao*, which is registered with the Guangzhou Marine Geological Survey Bureau. This expedition was the result of collaboration between the Guangzhou Marine Geological Survey and CUGB. The scientific goal of the cruise was to map gas hydrates using a marine EM method, while also using CSEM to determine the electrical structure 500
220 m below the seafloor. To achieve this, 20 previously developed OBEMs and a towed CSEM transmitter (Wang et al., 2017) were utilized during the cruise. To evaluate the overall performance of the developed receiver, two OBEMS were also used.

The Qiongdongnan region of the South China Sea is located 170 km southeast of Sanya. The seafloor is an ocean basin with a depth of 1700-1800m. Figure 5 shows a map of the experiment, which
225 included 22 receivers, where QH-R19 and QH-R21 indicate the two newly developed OBEMS, and other labels represent the existing OBEMs. All receivers were equipped with a USBL transponder. When the receiver started its descent to the seafloor, the transponder tracked its position. If the depth of the receiver did not change substantially, the location result was assumed to indicate the true position. After all receivers were deployed, two transmitter lines were towed for different waveforms: a single

230 square waveform at 8 Hz and multiple frequencies synthesized with a 0.5 Hz fundamental frequency. After 10 days on the seafloor, all 20 OBEMs and two OBEMS were successfully recovered. We estimated the MT responses (apparent resistivity and phase difference) using the robust estimate method (Egbert, 1997). To calculate the MT responses at site QH-R19, Figure 6 presents the respective computed MT responses for the site over a period from 10s to 10000s. The data quality is
235 excellent down to periods of approximately 10000s. At high frequencies we see the sea floor response for both modes asymptote to $1\Omega\text{m}$.

The CSEM data acquisition employed a towed CSEM transmitter that generated horizontal electrical
240 dipoles (HED) with a length of 300m, while the altimeter of the towed transmitter body was approximately 20~50m. The transmitters were used at a single frequency of 8Hz and multiple frequencies synthesized with a fundamental frequency of 0.5Hz. The transmitter was equipped with a depth sensor, an altimeter, and an acoustic transponder. The transmitter transmitted at 450 A. The OBEMS received CSEM data, following which the horizontal E-field and B-field component fast
245 Fourier transfer (FFT), current data FFT, instrument calibration, and field component rotation were performed. The Ex component of the site QH-R19 signal spectrum is presented in Figure 7. The result of the short time Fourier transform (STFT) shows the two towed CSEM lines (8 Hz towed line and 0.5Hz towed line) clearly. Figure 8 shows the MVO of the horizontal EM component at site QH-R19. The 8 Hz data are above the instrumental noise floor at a 3.5 km range.

250 After CSEM data acquisition using a towed transmitter source, seismic data acquisitions were carried out by testing the functionality of the OBEMS using an air gun as the source, the partial results of which are shown in Figure 9. The vertical peaks in each channel correspond to the acquisition of the reflected and refracted acoustic signals generated by the artificial source. The recordings show clear vibration signal arrivals, which demonstrate the proper functioning of all three geophone channels.

255 **5 Conclusions**

To achieve joint marine EM and seismic data acquisition, we installed an OBEMS based on an existing micro-OBE receiver, which consisted of two induction coils for horizontal magnetic field component measurement and a three-axis omni-directional geophone for recording movement of the seafloor in all directions, and assembled a USBL transponder for seafloor position tracking. The final system included
260 four electrodes, three geophones, two induction coils, two glass spheres, a USBL transponder, a motor drive release, an integrated ATM, a burn-wire release mechanism, a recovery beacon (LED, radio modem, VHF radio), and an expanded Wi-Fi module for data transfer. The data logger and battery are contained inside a 17-inch glass sphere. The proposed OBEMS architecture exhibited low noise, low clock drift, and low-power specifications. The OBEMS has been mechanically optimized to satisfy all
265 technical requirements for simultaneous acquisition of seismic and electromagnetic data. However, the following minor technical improvements will be made in future research:

- 1) The autonomy of the instrument will be extended to 60 days of data acquisition and 90 days spent on the seafloor.
- 2) A hydrophone will be installed to achieve a fully integrated all-in-one receiver.
- 270 3) The performance of the WiFi module will be enhanced.
- As these preliminary tests have shown, OBEMS technology is capable of high quality MT, CSEM, and artificial seismic data acquisition. The future instrument will add a hydrophone and lengthen the working time on the seafloor (2-3 months) to the existing advantages of the OBEMS (low cost, easy deployment, small size, high efficiency). This development will again be accomplished by cooperation
- 275 between GMGS and CUGB.

Data availability

The raw data of experiment are available upon request (ck@cugb.edu.cn).

Author contribution

280 KC design the new instrument and write the manuscript. MD is the project leader. ZLW and XHL provide idea and guidance, including the experiment. LZ designed and test electronics.

Competing interests

The authors declare that they have no conflict of interest.

Acknowledgements

The development of the OBEMS was supported by the National High Technology Research and Development Program of China (No. 2016YFC0303100, No. 2017YFF0105700) and the key project of the National Science Foundation of China (No. 61531001, No. 41804071). The development of the low-noise electrode and amplifier was supported by the Fundamental Research Funds for the Central Universities (No. 2652015403, 2652018265). Joint data acquisition was partially supported by the China Geological Survey (No. GZH-201100307). We also acknowledge the extensive support offered

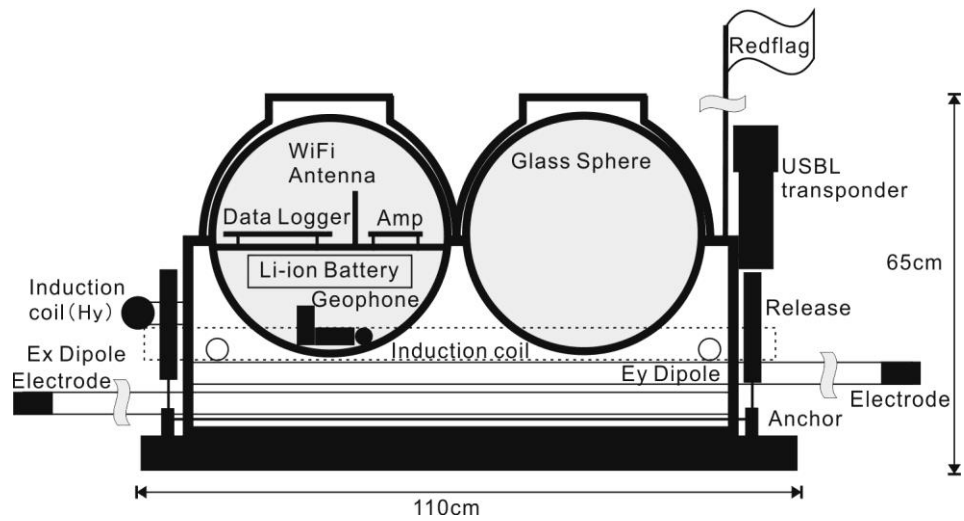
290 by the captain, ship's crew, and marine technicians of the R/V *Hai Yang Si Hao*, Dr. Jing for the EM data processing, Professor Zhao for technical help, and Dr. Tu for their helpful comments and support. The instruments were carefully manufactured and modified by Professor Zhang.

References

- Auffret, Y., Pelleau, P., Klingelhoefer, F., Geli, L., Crozon, J., Lin, J. Y., Sibuet J. : MicroOBS: A new generation of ocean bottom seismometer. *First break*, 22(7), 41-47, 2004.
- 295 Barsukov, P. O., and Fainberg, E. B.: Marine transient electromagnetic sounding of deep buried hydrocarbon reservoirs: principles, methodologies and limitations. *Geophysical Prospecting*, 65(3), 840-858, 2017.
- Chen, K., Deng, M., Luo, X., and Wu, Z.: A micro ocean-bottom E-field receiver. *Geophysics*, 82(5),
- 300 E233-E241, 2017.

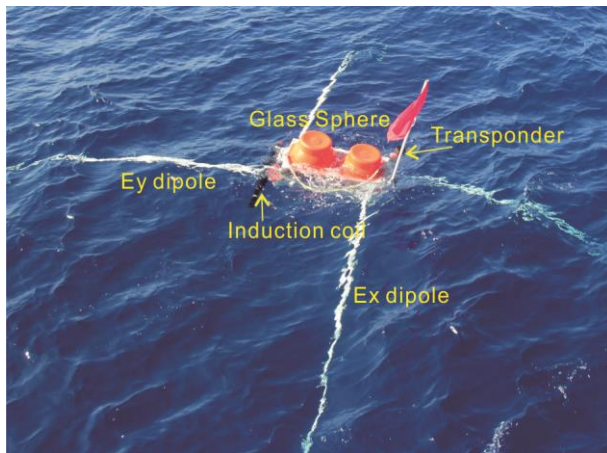
- Chen, K., Wei, W., Deng, M., Wu, Z., and Yu, G.: A new marine controlled-source electromagnetic receiver with an acoustic telemetry modem and arm-folding mechanism. *Geophysical Prospecting*, 63(6), 1420-1429, doi:10.1111/1365-2478.12297, 2015.
- Constable, S., and Heinson, G.: Hawaiian hot-spot swell structure from seafloor MT sounding. *Tectonophysics*, 389(1-2), 111-124, 2004.
- 305 Constable, S. C.: Review paper: Instrumentation for marine magnetotelluric and controlled source electromagnetic sounding. *Geophysical Prospecting*, 61, 505-532, 2013.
- Constable, S. C., and Srnka, L. J.: An introduction to marine controlled-source electromagnetic methods for hydrocarbon exploration. *Geophysics*, 72(2), WA3-WA12, 2007.
- 310 Deng, M., Wei, W., and Handong, T.: Collector For Seafloor Magnetotelluric Data. *Chinese Journal of Geophysics*, 2, 217-223, 2003.
- Ellingsrud, S., Eidesmo, T., Johansen, S., Sinha, M., MacGregor, L., and Constable, S. : Remote sensing of hydrocarbon layers by seabed logging (SBL): Results from a cruise offshore Angola. *The Leading Edge*, 21(10), 972-982, 2002.
- 315 Engemark, F., Mattsson, J., and Linfoot, J.: Simultaneous acquisition of towed EM and 2D seismic? A successful field test. *ASEG Extended Abstracts*, 2012(1), 1-4, 2012.
- QUASAR - GEOPHYSICAL TECHNOLOGIES :. <http://www.quasargeo.com/qmax.html>. Last access: 1 June 2019, 2019.
- Fanavoll S , Hesthammer J , Danielsen J , Stefatos, A. Controlled source electromagnetic technology and hydrocarbon exploration efficiency. *First Break*, 28(5), 2010.
- 320 Filloux, J. H.: An ocean bottom, D component magnetometer. *Geophysics*, 32(6), 978, 1967.
- Egbert, G. D., Robust multiple-station magnetotelluric data processing, *Geophys. J. Int.*, 130, 475– 496, 1997.
- Goswami, B. K., Weitemeyer, K. A., Bünz, S., Minshull, T. A., Westbrook, G. K., Ker, S., Sinha, M.
- 325 C.: Variations in pockmark composition at the Vestnesa Ridge: Insights from marine controlled source electromagnetic and seismic data. *Geochemistry, Geophysics, Geosystems*, 18(3), 1111-1125, 2017.
- Goswami, B. K., Weitemeyer, K. A., Minshull, T. A., Sinha, M. C., Westbrook, G. K., Chabert, A., Henstock, T. J., Ker, S.: A joint electromagnetic and seismic study of an active pockmark within the hydrate stability field at the Vestnesa Ridge, West Svalbard margin. *Journal of Geophysical Research: Solid Earth*, 120(10), 6797-6822, 2015.
- 330 ISL.: <http://www.islinc.com/solutions/advanced-sensor-technologies/>. Last access: 1 June 2019, 2016.
- Jing Jian-En , WU Z. L., Deng M. , Zhao Q.X. , Luo X.H. , Tu G.H. , Chen K., Wang M.: Experiment of marine controlled-source electromagnetic detection in a gas hydrate prospective region of the South China Sea. *Chinese Journal of Geophysics*, 59(7), 2564-2572, 2016.
- 335 Jürgen Mienert, Stefan Bünz, Stéphanie Guidard, Maarten Vanneste, Christian Berndt. Ocean bottom seismometer investigations in the Ormen Lange area offshore mid-Norway provide evidence for shallow gas layers in subsurface sediments. *Marine and Petroleum Geology*, 22, 287-297, 2005.
- Kasaya, T. G., T.-N.: A small ocean bottom electromagnetometer and ocean bottom electrometer system with an arm-folding mechanism (Technical Report). *Exploration Geophysics*, 40(1), 41-48, 340 2009.

- Key, K. : Marine Electromagnetic Studies of Seafloor Resources and Tectonics. *Surveys in Geophysics*, 33(1), 135-167, 2012.
- Key, K., and Constable, S.: Broadband marine MT exploration of the East Pacific Rise at 9 degrees 50 ' N. *Geophysical Research Letters*, 29(22), 2002.
- 345 Kodaira, S., Takahashi, N., Park, J.-O., Mochizuki, K., Shinohara, M., and Kimura, S.: Western Nankai Trough seismogenic zone: Results from a wide-angle ocean bottom seismic survey. *Journal of Geophysical Research*, 105(B3), 5887-5905, 2000.
- Mànuel, A., Roset, X., Rio, J. D., Toma, D. M., Carreras, N., Panahi, S. S., Benad, A. G., Owen, T., Cadena, J.: Ocean Bottom Seismometer: Design and Test of a Measurement System for Marine
350 Seismology. *Sensors*, 12(3), 3693-3719, 2012.
- Naif, S., Key, K., Constable, S., and Evans, R. L.: Water-rich bending faults at the Middle America Trench. *Geochemistry, Geophysics, Geosystems*, 16(8), 2582-2597, 2015.
- Panahi, S. S., Ventosa, S., and Cadena, J.: A Low-Power Datalogger Based on CompactFlash Memory for Ocean Bottom Seismometers. *IEEE Transactions on Instrumentation & Measurement*, 57(10),
355 2297-2303, 2008.
- QUASAR – GEOPHYSICALTECHNOLOGIES:. <http://www.quasargeo.com/qmax.html>. last access: 1 June 2019, 2019.
- Schwalenberg, K., Rippe, D., Koch, S., & Scholl, C.: Marine-controlled source electromagnetic study of methane seeps and gas hydrates at Opouawe Bank, Hikurangi Margin, New Zealand. *Journal of
360 Geophysical Research: Solid Earth*, 122(5), 3334-3350, 2017.
- Wang, M., Deng, M., Wu, Z., Luo, X., Jing, J., and Chen, K. :The deep-tow marine controlled-source electromagnetic transmitter system for gas hydrate exploration. *Journal of Applied Geophysics*, 137, 138-144, 2017.
- Wang, M., Deng, M., Zhao, Q., Luo, X., and Jing, J.: Two types of marine controlled source
365 electromagnetic transmitters. *Geophysical Prospecting*, 63(6), 1403-1419, 2015.
- Wei, W., Deng, M., and Wen, Z.: Experimental Study of Marine Magnetotelluric in Southern Huanghai. *Chinese Journal of Geophysics*, 52(2), 440-450, 2009.
- Weitemeyer, K. A., Constable, S., and Tr řu, A. M.: A marine electromagnetic survey to detect gas hydrate at Hydrate Ridge, Oregon. *Geophysical Journal International*, 187(1), 45-62, 2011.
- 370 Weitemeyer, K. A., Constable, S. C., Key, K. W., and Behrens, J. P.: First results from a marine controlled-source electromagnetic survey to detect gas hydrates offshore Oregon. *Geophysical Research Letters*, 33(3), L03304, 2006.
- Zhang, L., Baba, K., Liang, P., Shimizu, H., and Utada, H.: The 2011 Tohoku Tsunami observed by an array of ocean bottom electromagnetometers. *Geophysical Research Letters*, 41(14), 4937-4944, 2014.
- 375 Zhdanov, M. S., Endo, M., Čuma, M., Linfoot, J., Cox, L. H., and Wilson, G. A.: The first practical 3D inversion of towed streamer EM data from the Troll field trial. In *Seg Technical Program Expanded*, 2012,1-5,2012.



385

Fig. 1 Schematic diagram of the ocean bottom electromagnetic receiver and seismometer (OBEMS). Diagram shows the structural design inside the glass sphere, with omni-directional geophones in the lowest layer, then the Li-ion battery sets, Acoustic Telemetry Modem (ATM), and the data logger. All print circuit boards are covered with a magnetic shielding box. Ferrite sheets, with 0.01mm thick film on one side and 0.02mm thick adhesive tape on the other, were glued inside the shielding box. These ferrite sheets function primarily as suppressors, blocking EM noise at lower frequencies and absorbing it at higher frequencies.



390

Fig. 2 Photograph of the OBEMS while in the water, ascending to the sea surface after release. The length of the electrode dipole is 12m.

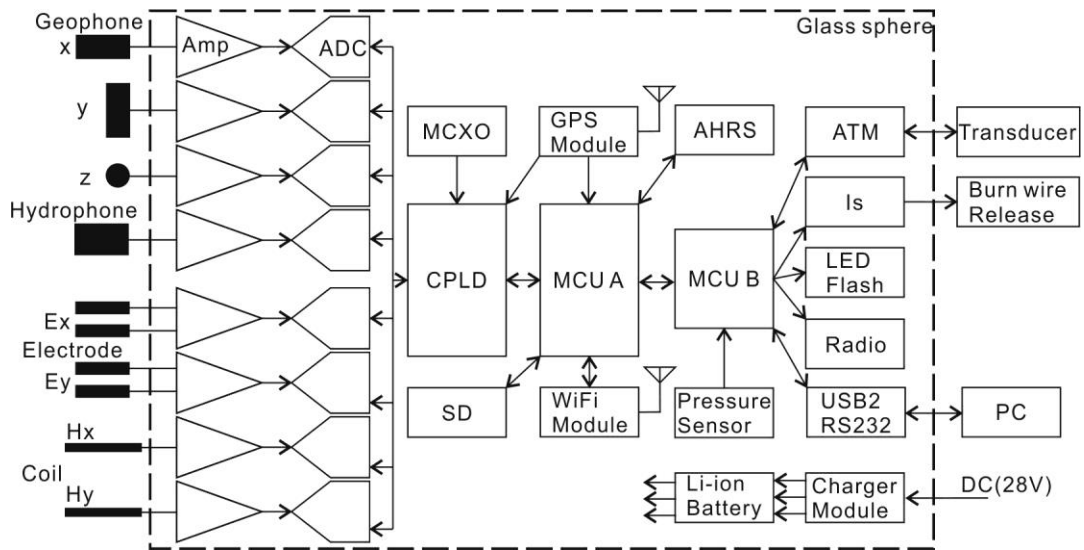
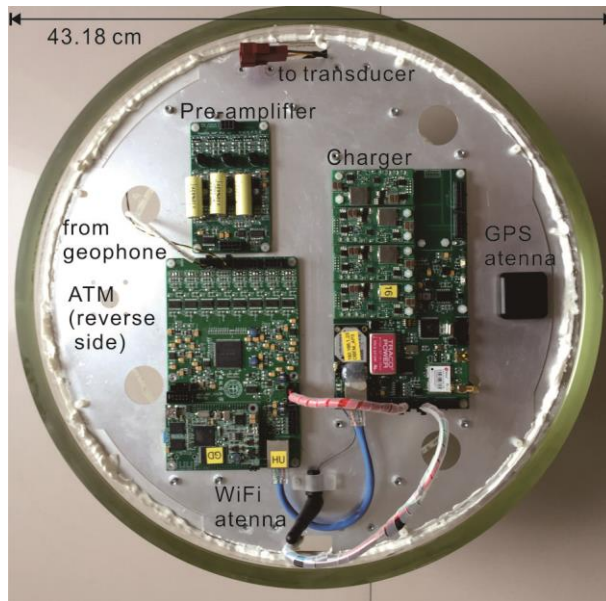


Fig. 3 Circuit diagram of the OBEMS data logger. It contains EM and seismic sensors, an amplifier, an analog to digital converter, controller, storage card, clock module, battery, charger, beacon, acoustic telemetry module (ATM) and attitude heading reference system (AHRS). In this preliminary design, the ATM, burn wire release, USBL, and relay release are all designed for release.



405 **Fig. 4** Photo of the data logger installed in the glass sphere. Under the aluminum board, an ATM, Li-ion battery set, and three-axis geophone are fixed. After circuit assembly, magnetic shields cover the three print circuit boards to decrease sensor disturbance.

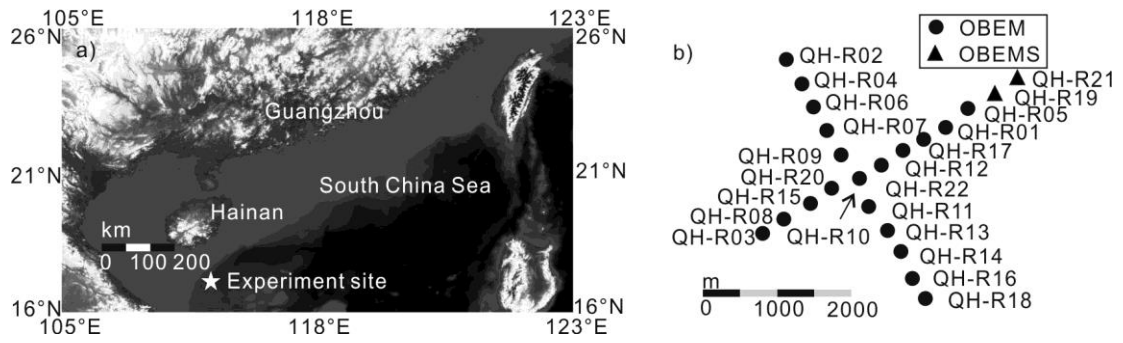


Fig. 5 Photograph of the offshore experiment area and site map with all locations marked. The map is powered by Global Mapper.

415

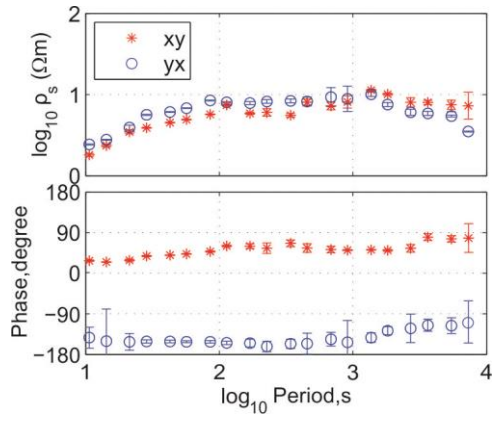


Fig. 6 Apparent resistivity (top) and phase (bottom) curves calculated with the OBEMS E-field and B-field at site QH-R19. The red star indicates the xy component and the blue circles indicate the yx component.

420

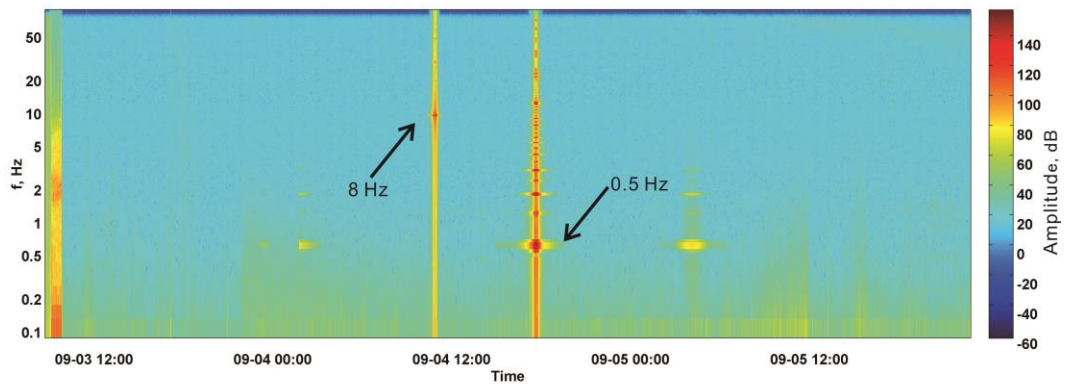


Fig. 7 Short time Fourier transform results of the CSEM signal from the horizontal electrical field components.

425

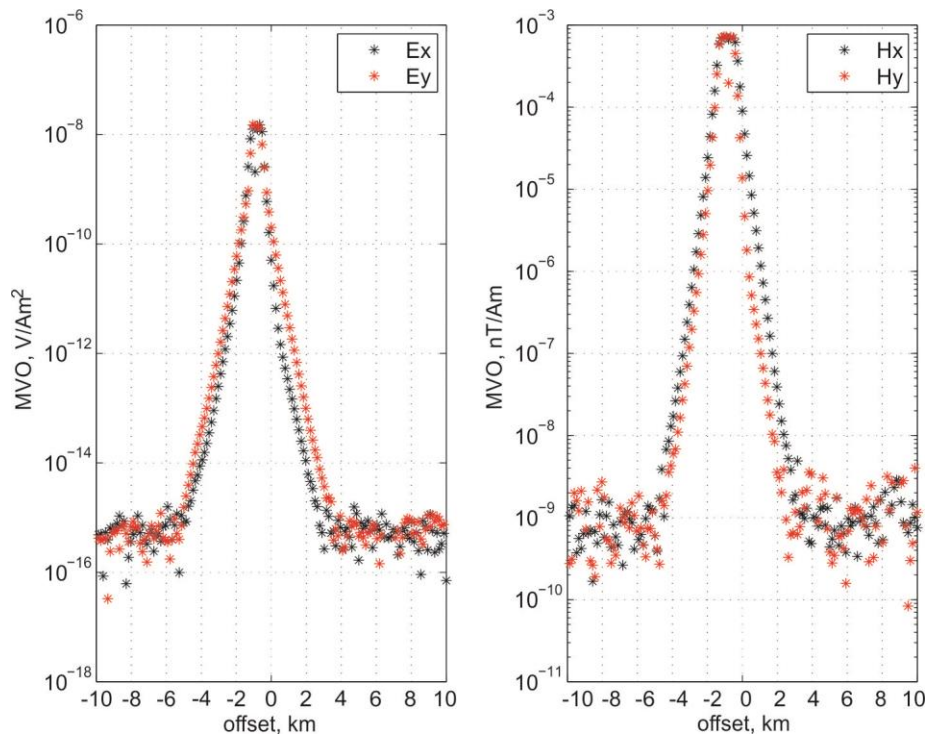
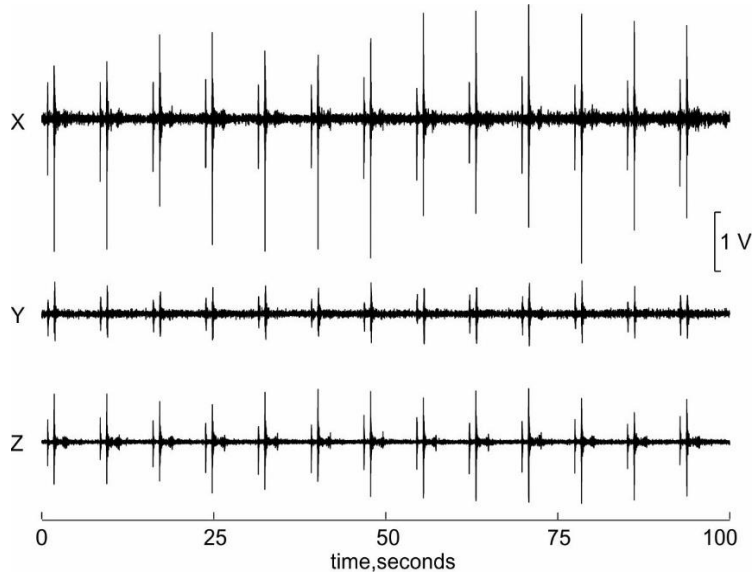


Fig.8 Magnitude versus offset, E component and H component (site: QH-R19, frequency: 8 Hz).



435 **Fig. 9** Seismic data acquisition test results in real environmental conditions from the OBEMS at test site QH-R21. (a) First horizontal component, (b) second horizontal component, and (c) vertical geophone component.

Table 1 Technical specifications of the ocean bottom electromagnetic receiver and seismometer (OBEMS)

Channels	7 $E_x \setminus E_y$, Geophone (x,y,z), H_x , H_y
Sensor Type	Electrode: Ag/AgCl Magnetic sensor: induction coil Geophone: Triaxial, Orthogonal, omnidirectional moving coil
-3dB band width	E field: 100 s~100 Hz Induction coil :0.1 Hz~500 Hz Geophone: 10 Hz~300 Hz
Maximum battery lifetime	30 days
Memory	32 GB SD card (upgrade 128 GB)
Release mechanism	USBL motor drive release and burn wire release
Weight	114 kg in air (exclude anchor) -32 kg in water
Electrode dipole	12 m
Dynamic range	E field channel :110 dB@, B filed channel: 130dB@fs=1000Hz Seismic channel:130dB@fs=1000Hz
Position in water	USBL responder
Sensitivity	Geophone: 78.5 V/m/s at 15 Hz Induction coil: 0.3 V/nT
Gain preamplifier	E field channel :480 to 30720 step 2 B filed channel: 0.4 to 25.6 step 2 Geophone: 20 to 56dB step 6dB
Noise level	E field: 0.1 nV/m/rt (Hz) @ 1 Hz B filed: 0.1pT/rt(Hz) @ 1 Hz
Time drift error	Less than 2 ms/day
Maxim Work water depth	4000 m
User interface	USB & WiFi (transfer data rate 3 MB/s)